ISSN 1066-3622, Radiochemistry, 2015, Vol. 57, No. 4, pp. 348–355. © Pleiades Publishing, Inc., 2015.
Original Russian Text © S.V. Stefanovsky, O.I. Stefanovskaya, S.E. Vinokurov, S.S. Danilov, B.F. Myasoedov, 2015, published in Radiokhimiya, 2015, Vol. 57, No. 4, pp. 295–301.

Phase Composition, Structure, and Hydrolytic Durability of Glasses in the Na_2O–Al_2O_3–(Fe_2O_3)–P_2O_5 System at Replacement of Al_2O_3 by Fe_2O_3

S. V. Stefanovsky*[a], O. I. Stefanovskaya[a], S. E. Vinokurov[b], S. S. Danilov[b], and B. F. Myasoedov[a,b]

[a] *Frumkin Institute of Physical Chemistry and Electrochemistry, Russian Academy of Sciences, Leninskii pr. 31, korp. 4, Moscow, 119071 Russia*
[b] *Vernadsky Institute of Geochemistry and Analytical Chemistry, Russian Academy of Sciences, ul. Kosygina 19, Moscow, 119991 Russia*
** e-mail: serge.stefanovsky@yandex.ru*

Received December 5, 2014

Abstract—Samples of sodium aluminum iron phosphate glasses of the composition (mol %) 40 Na_2O, (20 – x) Al_2O_3, x Fe_2O_3, 40 P_2O_5 (series I) and 35 Na_2O, (20 – x) Al_2O_3, x Fe_2O_3, 45 P_2O_5 (series II) were synthesized. The phase composition and structure of the samples obtained were determined by X-ray diffraction and IR spectroscopy. At equimolar replacement of Al_2O_3 by Fe_2O_3, the structure of the quenched glasses of series I does not change appreciably, in contrast to glasses of series II. Annealing of the glasses leads to their partial devitrification with segregation of crystalline aluminum iron phosphate phases. Glasses of series I with up to 10 mol % Al_2O_3 replaced by Fe_2O_3 exhibit the highest hydrolytic durability: The leach rates of Na, Al, Fe, and P from the samples are within (4–10) × 10^{-8} g cm^{-2} day^{-1}, meeting the requirements of GOST (State Standard) R 50926–96. Thus, glasses with approximately equal molar concentrations of Al_2O_3 and Fe_2O_3 are the most resistant to crystallization and hydrolysis.

Keywords: sodium aluminum phosphate glasses, stability, leaching

DOI: 10.1134/S1066362215040037

Vitrification is today the only commercially implemented technology for management of high-level waste (HLW) from reprocessing of spent nuclear fuel (SNF) and implementation of military programs [1]. In the majority of countries (France, the United States, the United Kingdom, Germany, Japan, India, South Korea), sodium borosilicate glass is used for HLW immobilization, and in Russia sodium aluminophosphate glass is used. Aluminophosphate glass, compared to borosilicate glass, is capable of incorporating larger amounts of polyvalent transition elements, sulfates, and chlorides, but is less resistant to crystallization and is characterized by the shorter interval of variation of the melt viscosity [2–4]. Numerous attempts were made to improve glasses on aluminum phosphate base, e.g., by introducing boron and silicon oxides [5, 6].

Initially, the choice of aluminophosphate glass for use in Russia was governed by the need for immobilization of HLW of mainly sodium aluminate composition from reprocessing of SNF with aluminum cladding. The composition range (wt %) was determined for preparing at temperatures of up to 1000°C chemically durable sodium aluminophosphate glasses resistant to devitrification and incorporating up to 10 wt % HLW oxides: 24–27 Na_2O, 20–24 Al_2O_3, and 49–56 P_2O_5 [2]. It should be noted in this connection that some batches of the new HLW types or "historical" wastes from the defense activity, stored in stainless steel vessels at the Mayak Production Association, contain large amount of iron along with sodium and aluminum [7]. Therefore, the glasses that will be obtained by vitrification of such wastes will actually be sodium aluminum iron phosphate glasses.

The effect of iron oxide on the structure and properties of sodium aluminophosphate glasses has been studied insufficiently. Oziraner et al. [2] showed that partial replacement of Al_2O_3 by Fe_2O_3 in glasses with the molar ratio Na : P = 0.9–1.4 influenced their chemical durability insignificantly. It was also found that annealing of the glasses at 400–500°C led to their

Table 1. Calculated compositions (mol %) of glass samples of series I [40 Na_2O, (20 – x) Al_2O_3, x Fe_2O_3, 40 P_2O_5] and I [35 Na_2O, (20 – x) Al_2O_3, x Fe_2O_3, 45 P_2O_5]

Component	Series I					Series II				
	I-1 (x = 0)	I-2 (x = 5)	I-3 (x = 10)	I-4 (x = 15)	I-5 (x = 20)	II-1 (x = 0)	II-2 (x = 5)	II-3 (x = 10)	II-4 (x = 15)	II-5 (x = 20)
Na_2O	40	40	40	40	40	35	35	35	35	35
Al_2O_3	20	15	10	5	0	20	15	10	5	0
Fe_2O_3	0	5	10	15	20	0	5	10	15	20
P_2O_5	40	40	40	40	40	45	45	45	45	45

partial or complete crystallization depending on the iron content. In the process, the chemical stability did not change noticeably, but the mechanical strength decreased [2, 8]. Mogus-Milanković et al. [9] studied the structure of glasses of the series, mol %: 20 Na_2O, x Al_2O_3, (20 – x) Fe_2O_3, 60 P_2O_5. It was found that an increase in the Fe_2O_3 content of the glasses led to a decrease in the degree of binding of the glass structural network and to an increase in its tendency to crystallization; however, the Na_2O content of these glasses was approximately 2 times lower than that of the glasses studied in [2].

We chose for the studies glasses of two base compositions (wt %/mol %), one of which is within the region examined in [2] (24.3/40.0 Na_2O; 20.0/20.0 Al_2O_3; 55.7/40.0), and the other is beyond this region (20.5/35.0 Na_2O; 19.2/20.0 Al_2O_3; 60.3/45.0 P_2O_5). In the glass formulations, Al_2O_3 was replaced to different extents by Fe_2O_3.

This study was aimed at determining how the equimolar replacement of Al_2O_3 by Fe_2O_3 influences the structure, phase composition, and hydrolytic stability of glass materials of the following series (mol %): 40 Na_2O, (20 – x) Al_2O_3, x Fe_2O_3, 40 P_2O_5 (series I) and 35 Na_2O, (20 – x) Al_2O_3, x Fe_2O_3, 45 P_2O_5 (series II).

EXPERIMENTAL

The starting compounds for preparing glass samples were sodium and aluminum metaphosphates [$NaPO_3$ and $Al(PO_3)_3$], aluminum and iron oxides (Al_2O_3 and Fe_2O_3), and ammonium dihydrogen orthophosphate ($NH_4H_2PO_4$); all the chemicals were of pure or analytically pure grade. Mixtures of chemicals were placed in quartz crucibles, heated over a period of 5 h to the founding temperature of 1300°C, and kept at this temperature for 30 min. Glass samples whose calculated composition is given in Table 1 were obtained by quenching a part of the melt by its casting onto a stainless steel plate (samples denoted by index q) and by annealing the remaining melt by cooling in the switched-off furnace at a mean rate of approximately 100 deg h^{-1} (samples denoted by index a).

The chemical composition of the synthesized glass samples was determined by X-ray fluorescence analysis with a PW-2400 spectrometer (Philips Analytical B.V., Netherlands) with Philips Super Quantitative & IQ Software 2001.

The phase composition of the samples was studied by X-ray diffraction (XRD) analysis with an Empyrean X-ray diffractometer (Ni-filtered CuK_α radiation).

The structure of the anionic motif of the structural network of the glasses was determined by Fourier transform IR spectrometry with a Shimadzu IR Prestige 21 spectrophotometer. The powdered glass samples were pelletized with KBr.

The hydrolytic durability of the glasses was evaluated in accordance with GOST (State Standard) R 52126–2003. Glass samples were finely milled, the powder fraction with the particle size in the range 0.16–0.25 mm was taken, and the powder was placed in Teflon vessels, poured over with double-distilled water, and kept at 23 ± 2°C for 28 days with intermittent replacement of the contact solution. The specific surface area of the glass samples was determined by the BET method. Elemental analysis of the solutions after leaching was performed by inductively coupled plasma atomic emission spectrometry (ICAP 6500 spectrometer).

RESULTS AND DISCUSSION

The chemical compositions of the synthesized glass samples of the two series were in good agreement with the calculated compositions (Table 1), with the SiO_2 impurity not exceeding 0.5 wt %.

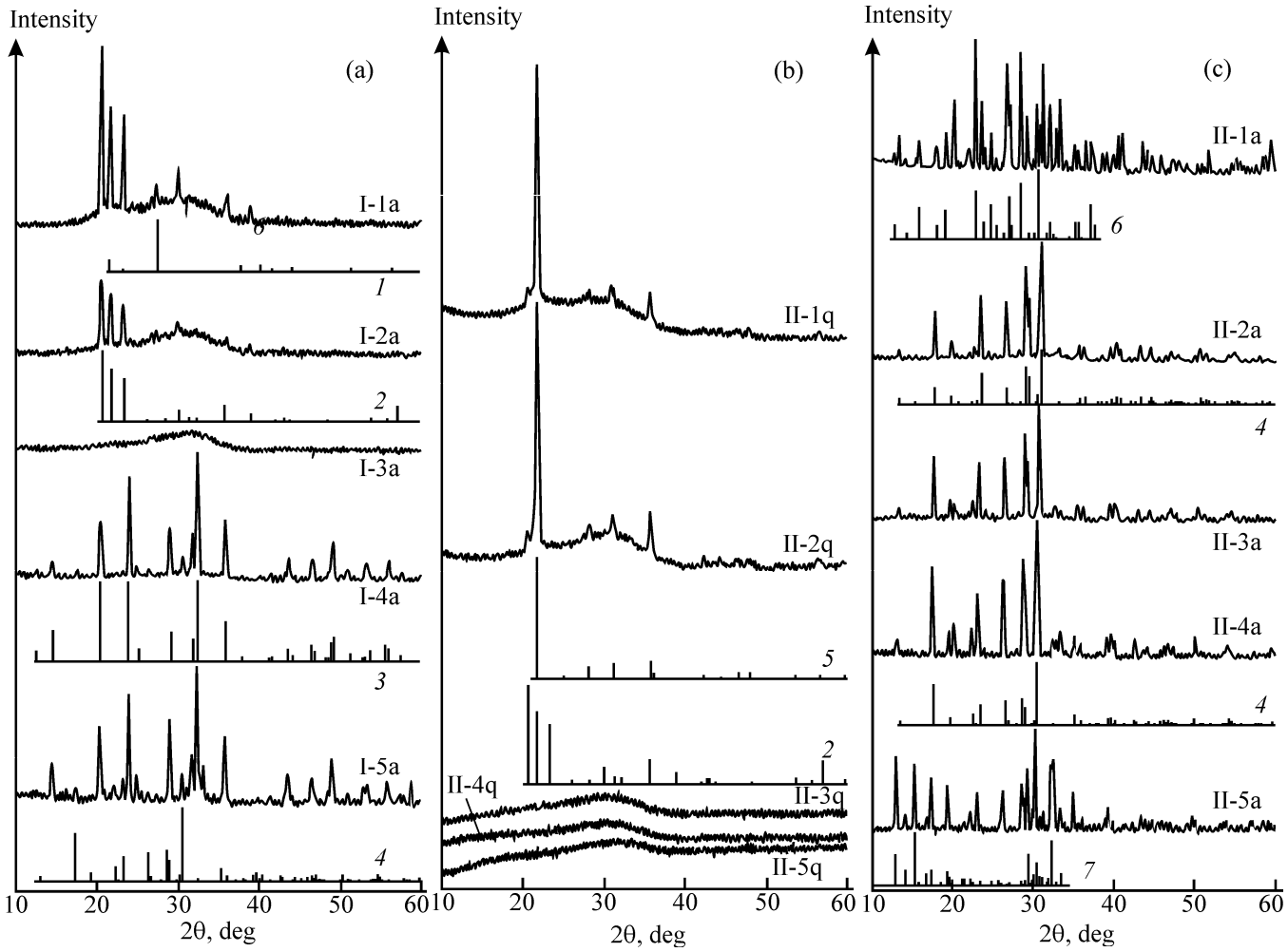

Fig. 1. X-ray diffraction patterns of the synthesized glass samples: (a) annealed samples of series I, I-1a–I-5a; (b) quenched samples of series II, II-1q–II-5q; and (c) annealed samples of series II, II-1a–II-5a. X-ray diffraction patterns given for comparison: (*1*) berlinite (α-$AlPO_4$), (*2*) phosphotridymite (γ-$AlPO_4$), (*3*) $Na_3Fe_2(PO_4)_3$, (*4*) $NaFeP_2O_7$, $Na(Al,Fe)P_2O_7$, (*5*) phosphocristobalite (β-$AlPO_4$), (*6*) $Na_7Al_4(P_2O_7)_4PO_4$, and (*7*) $Na_7Fe_3(P_2O_7)_4$.

Phase Composition of Samples

The results of XRD analysis showed that samples of series I, prepared by quenching of the melts (samples I-1q–I-5q), were X-ray amorphous and homogeneous. After the annealing, samples of this series partially crystallized, except sample I-3a, which remained amorphous (Fig. 1a). As we found, samples I-1a and I-2a are constituted by the matrix glass phase and aluminum orthophosphate, mainly in the form of phosphotridymite (γ-$AlPO_4$), with berlinite (α-$AlPO_4$) present in small amounts as impurity (Fig. 1a). Samples I-4a and I-5a, in which Al_2O_3 is replaced to 15 and 20 mol % by Fe_2O_3, are largely crystallized, and their major phase is sodium iron orthophosphate (in sample I-4a, probably, with an impurity of Al_2O_3), and the impurity phases are sodium iron pyrophosphate $NaFeP_2O_7$ and hematite Fe_2O_3.

Quenched samples II-1q and II-2q underwent partial crystallization (Fig. 1b), with aluminum orthophosphate in the phosphocristobalite form (β-$AlPO_4$) as major phase and in the phosphotridymite form as minor phase. Samples II-3q–II-5q remained amorphous (Fig. 1b). After annealing, all the samples of series II underwent crystallization (Fig. 1c), and the major phase in them was sodium aluminum iron pyrophosphate of the composition $NaAl_{1-x}Fe_xP_2O_7$: from $NaAlP_2O_7$ in sample II-1q to $NaFeP_2O_7$ in sample II-5q. Sample II-1q also contained an additional phase of sodium aluminum ortho–pyrophosphate similar in the X-ray diffraction parameters to $Na_7Al_4(P_2O_7)_4PO_4$ [10] or $Na_6Al_2(P_2O_7)_3$ (possibly, $Na_2Al_{0.67}P_2O_7$) [11], and sample II-5q , an additional phase of sodium iron pyrophosphate $Na_7Fe_3(P_2O_7)_4$ [12].

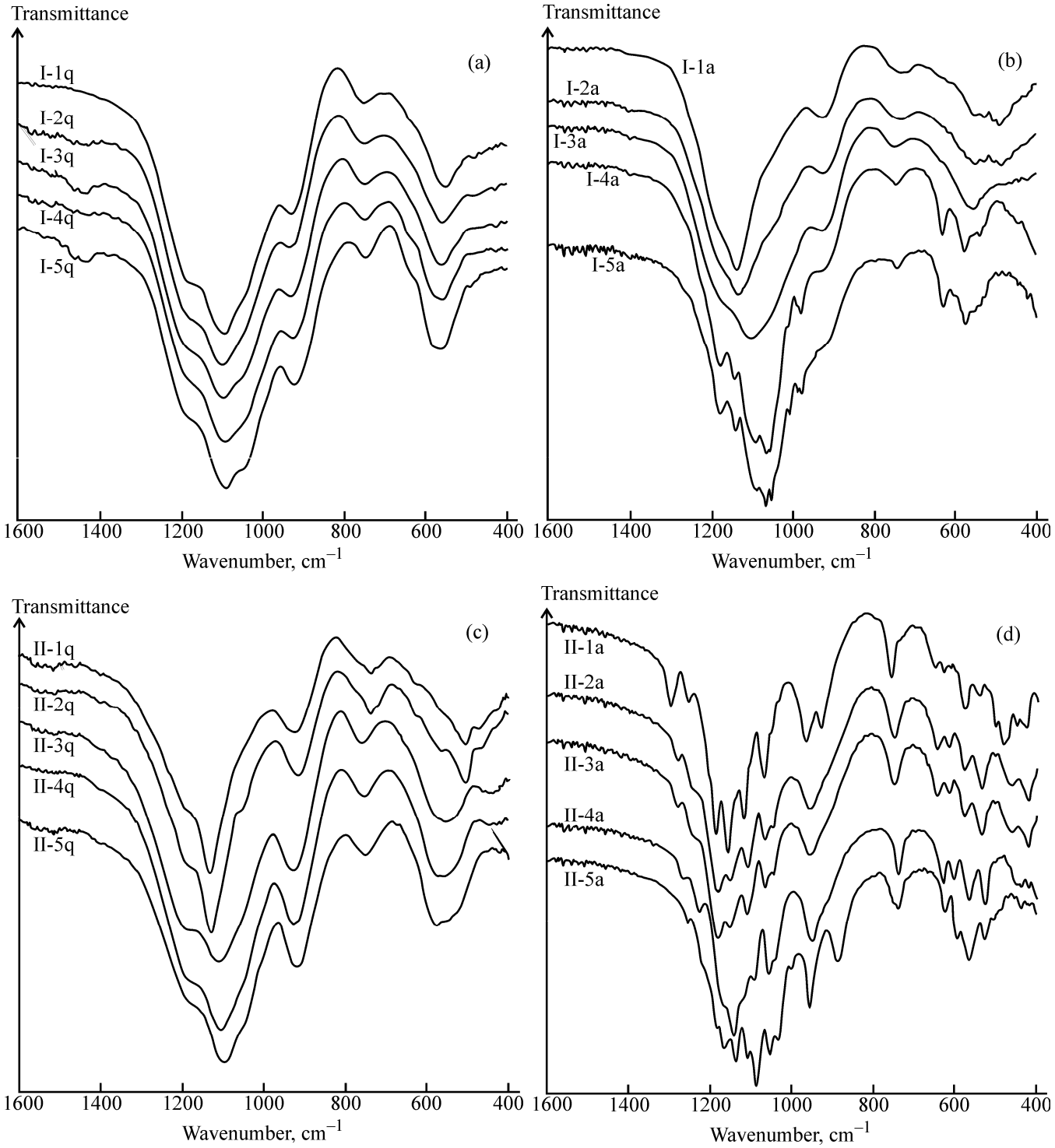

Fig. 2. IR spectra of glasses of series I [(a) quenched and (b) annealed] and II [(c) quenched and (d) annealed].

Structure of the Anionic Motif in the Glasses

The structure of the anionic motif of the glass network in the synthesized samples was determined from the IR spectra (Figs. 2a–2d).

In the spectra of quenched samples of series I (Fig. 2a, Table 2), the absorption bands in the range 400–700 cm^{-1} are mainly caused by bending vibrations in phosphorus–oxygen groups, and also by stretching vibrations of the Al–O and Fe–O bonds in the AlO_n

Table 2. Positions of the absorption band maxima (cm^{-1}) in the IR spectra of quenched glass samples of series I

I-1q	I-2q	I-3q	I-4q	I-5q	Assignment
483	484	482	490	477	δ P–O–P, ν_s FeO_4, ν_s AlO_6
516 540	516 553	516	 529 545	 530	δ_{as} PO_3, δ_s PO_4, ν_{as} FeO_4
569	573	559	560	560	δ_{as} PO_4, ν_{as} AlO_6
596	590	596	584	588	ν_{as} P–O–Fe
627	628	633	635	631	ν_s AlO_4
727 755	725 754	715 750	 749	 753	ν_s P–O–P, ν_{as} AlO_4
912	921	917	920	915	ν_{as} P–O–P
1003	989	981	982	980	ν_s PO_4
1059	1033	1032	1025	1025	ν_{as} PO_4
1102	1089	1098	1084	1088	ν_s PO_3, ν_s P–O–Al
1169	1175	1170	1175	1172	ν_{as} PO_3, ν_{as} P–O–Al

and FeO_n polyhedra. The absorption bands in the ranges 700–800 and 900–950 cm^{-1} belong, respectively, to the symmetric and antisymmetric stretching vibrations of the bridging P–O–P and P–O–Al bonds linking the PO_4 tetrahedra with each other and with AlO_4 tetrahedra. The absorption bands in the ranges 950–1050, 1050–1150, 1150–1250, and 1250–1350 cm^{-1} correspond to vibrations of the O–P–O bonds in the PO_4 tetrahedra with 0, 1, 2, and 3 bridging oxygen atoms, respectively, and those in the range 1300–1400 cm^{-1}, to vibrations of P=O double bonds [13–23]. In the ranges 3400–3800 and 1450–1600 cm^{-1}, there are also weak absorption bands corresponding, respectively, to stretching and bending vibrations of the H–O–H bonds in molecules of adsorbed and structurally bound water. Thus, on replacement of Al_2O_3 by Fe_2O_3, the spectra of quenched samples of series I undergo no cardinal changes; the positions of the band maxima in the spectra remain essentially unchanged.

As for annealed samples of series I, only the spectrum of sample I-3a (Fig. 2b) has the shape typical of the glassy state. The spectra of samples I-1a and I-2a are characterized by appreciable broadening of the absorption bands relative to the spectra of the quenched samples, and in the spectra of samples I-4a and I-5a the bands are split owing to lifting of the degeneracy of the stretching and bending vibrations as a result of the glass crystallization. The spectra of samples I-1a and I-2a are superpositions of the spectra of the crystalline $AlPO_4$ phase, mainly in the phosphotridymite form, and of the glass phase, which is consistent with the XRD data. It was noted previously [20] that, for phosphotridymite, the positions of the band maxima are as follows: 1141 (A_1), 505–451 (F_2), 372 (E), 735–525 (vibrations of Al pseudolattice), and 226 cm^{-1} (lattice vibrations, librations). The other bands belong to the vibrations of bonds in the phosphorus–oxygen network of the glass, in particular, the bands at 900–950 and 700–750 cm^{-1} (ν_{as} and ν_s vibrations of bridging P–O–P bonds), a shoulder at 950–1000 cm^{-1} (stretching vibrations of O–P–O bonds, mainly in orthophosphate groups), and bands below 700 cm^{-1} (δ PO_4). The spectrum of amorphous sample I-3a (Fig. 2b) suggests the presence of a noticeable amount of pyrophosphate groups (Q^1 tetrahedra, absorption maximum at 1112 cm^{-1}), which is quite consistent with its chemical composition. In the spectra of I-4a and I-5a, there are the absorption bands belonging to vibrations of both ortho- and pyrophosphate groups in the crystals of sodium iron ortho- and pyrophosphate, and also the bands of the residual glass phase (Fig. 2b).

Quenched samples of series II, II-1q and II-2q, contain a crystalline phase, which is manifested in the spectra in narrowing of the stretching and splitting of the bending vibration bands of phosphorus–oxygen groups (Fig. 2c). The positions of the absorption bands belonging to vibrations of the bonds in these samples correspond to those in phosphocristobalite: 1125–1126 (A_1); 735, 624, and 566 (vibrations in the aluminate pseudolattice); 495 and 465 cm^{-1} (E) [20]. They overlap with the vibration bands of the phosphorus–oxygen

Table 3. Positions of the absorption band maxima (cm^{-1}) in the IR spectra of annealed glass samples of series II

II-1a	II-2a	II-3a	II-4a	II-5a	Assignment
425 w	422 m	422 m	422 w	421 w	δ P–O–P, ν_s FeO_4, ν_s AlO_6
477 m, 470 m, 455 w	469 m, 459 m	468 m, 458 m	448 w, 439 w	439 w	δ_s PO_3, ν_{as} FeO_6, ν_{as} AlO_6, ν_s P–O–Fe
500 w	504 w	504 w	505 sh	510 sh, 488 sh	δ_{as} PO_3, ν_{as} FeO_4
541 w	538 m	536 m	529 m	530 m	δ_s PO_4, ν_s AlO_5
576 m	578 m	578 m	567 m	570 s	δ_{as} PO_4, ν_{as} AlO_6
629 w, 612 sh	616 w	616 w	603 s	598 w	ν_{as} P–O–Fe, ν_{as} AlO_5
651 w	645 m	645 m	632 m	628 m	ν_s AlO_4
758 s	752 s	752 s	742 s	754 w, 740 s	ν_s P–O–P, ν_{as} AlO_4
931 w 968 m	961 s	961 s	956 s	890 s 960 s	ν_s PO_4, ν_{as} P–O–P
1055 sh, 1035 sh	1048 w	1048 w	1044 w	1035 w	ν_s PO_3
1069 s	1068 s	1068 s	1058 s	1056 s	ν_{as} PO_4
1120 s	1111 s	1111 s	1120 sh, 1095 w	1112 w, 1091 vs	ν_s PO_3
1159 vs	1156 s	1156 s	1145 vs	1140 vs	ν_{as} PO_3
1189 vs	1185 vs	1185 vs	1167 w	1187 w 1171 s	ν_s PO_2, ν_s P–O–Al
1254 w	~1240 sh	~1240 sh	1228 w	~1220 sh	ν_{as} PO_2, ν_{as} P–O–Al
1300 m	1282 w	1282 w	1267 w	1258 w	ν P=O

groups in the glass phase of mainly pyrophosphate composition. With further equimolar replacement of Al_2O_3 by Fe_2O_3 (samples II-3q–II-5q), the band at 950–1300 cm^{-1} becomes broader, and its maximum shifts toward smaller wavenumbers (to ~1100 cm^{-1}), suggesting an increase in the fraction of orthophosphate groups; the intensity of the bands at 850–950 and 700–800 cm^{-1} somewhat increases, and the absorption in the range 550–600 cm^{-1}, and also below 500 cm^{-1}, caused by the contribution of the bending vibrations of the phosphorus–oxygen groups and stretching vibrations of the aluminum–oxygen and iron–oxygen groups in the glass phase, increases.

In the spectra of annealed samples of series II (Fig. 2d), there is a large number of absorption bands belonging to vibrations of bonds in the phosphorus–, aluminum–, and iron–oxygen groups. Tentative assignment of the absorption bands, based on the data from [18–20], is given in Table 3. As can be seen, the spectra mainly consist of absorption bands belonging to vibrations of bonds in the pyro- and orthophosphate groups in the structure of the crystalline phases. The presence of even weak additional bands in the range below 700 cm^{-1} suggests assignment of at least a part of them to vibrations of the Al–O and Fe–O bonds in the structure of the crystalline phase and residual glass phase, including the bonds linking the PO_4 tetrahedra with the AlO_4/AlO_6 or FeO_4/FeO_6 polyhedra.

Hydrolytic Durability of Glasses

The results of studying the hydrolytic durability of quenched samples of glasses of series I are shown in Fig. 3. The initial leach rates of sodium, aluminum, iron, and phosphorus from the glass powders with the specific surface area of approximately 0.5 $m^2\ g^{-1}$ are in the range from (2–5) × 10^{-7} to (1–2) × 10^{-6} g cm^{-2} day^{-1}. The leach rates decrease with time, and on the 28th day of contact of samples I-1q–I-3q with water they become equal to (4–10) × 10^{-8} g cm^{-2} day^{-1}. Only the leach rates of Na from high-iron samples I-4q and I-5q, and also of Fe and P from sample I-5q are somewhat higher: (2–5) × 10^{-7} g cm^{-2} day^{-1}. For iron and, to a lesser extent, for aluminum the leach rate from samples I-4q и I-2q, respectively, slightly increases in the first 3–4 days of contact with water, which may be due to the release of these elements from the surface layer of the samples.

Replacement of up to 50% of Al_2O_3 by Fe_2O_3 enhances the hydrolytic durability of the glasses. In the first 7 days of contact with water, the Na leach rate is minimal for sample I-3q, and then it becomes lower for sample I-2q. With further replacement of Al_2O_3 by Fe_2O_3, the leach rate of the elements increases again. The maximal hydrolytic durability of the glass samples with 5 and 10 mol % Fe_2O_3 is probably due to the formation of a highly polymerized network of the PO_4

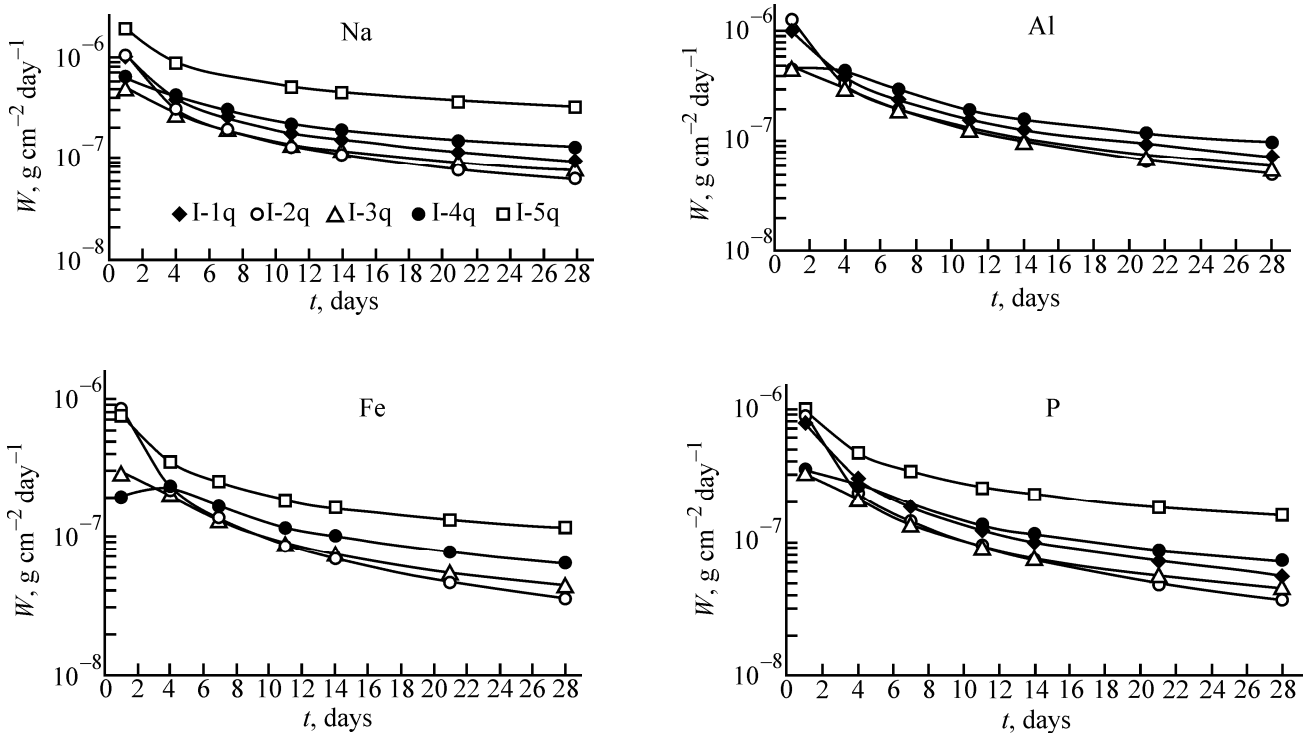

Fig. 3. Leach rates (W) of sodium, aluminum, iron, and phosphorus from quenched samples of glasses of series I, I-1q–I-5q.

and AlO_4 tetrahedra and FeO_6 octahedra, which are the structure-forming nodes near which the Na^+ and $Fe^{2+/3+}$, playing the role of network modifiers, are localized. This fact my be responsible in part for similar leach rates of the ions from the examined glass samples.

The leach rates that we determined for the constituent elements of the glasses are close to those obtained previously [2]. The hydrolytic durability of all the glass samples studied meets the requirements of GOST (State Standard) R 50926–96 and NP (Federal Norms and Regulations in the Field of the Use of Atomic Energy) 019–2000.

Thus, our study shows that, among the synthesized samples of sodium aluminum iron phosphate glasses of two series, the samples containing equal molar concentrations of Al_2O_3 and Fe_2O_3 (~10 mol %) exhibit the highest resistance to crystallization and hydrolysis.

ACKNOWLEDGMENTS

The authors are grateful to M.I. Kadyko (Frumkin Institute of Physical Chemistry and Electrochemistry, Russian Academy of Sciences) for recording the IR spectra.

The study was financially supported by the Russian Science Foundation (project no. 14-13-00615).

REFERENCES

1. Dmitriev, S.A. and Stefanovsky, S.V., *Obrashchenie s radioaktivnymi otkhodami* (Radioactive Waste Management), Moscow: Ross. Khimiko-Tekhnol. Univ. im. D.I. Mendeleeva, 2000.
2. Oziraner, S.N., Minaev, A.A., Kuznetsov, D.G., and Prokhorova, N.P., in *Materialy IV nauchno-tekhnicheskoi konferentsii SEV* (Proc. IV COMECON Scientific and Technical Conf.), Moscow, Dec. 22–23, 1976, Moscow: Atomizdat, 1978, pp. 94–102.
3. Brezhneva, N.E., Minaev, A.A., and Oziraner, S.N., *Scientific Basis for Nuclear Waste Management*, McCarthy, G. J., Ed., New York: Plenum, 1979, vol. 1, pp. 43–50.
4. *Fosfatnye stekla s radioaktivnymi otkhodami* (Phosphate Glasses with Radioactive Wastes), Vashman, A.A. and Polyakov, A.S., Eds., Moscow: TsNIIAtominform, 1997.
5. Medvedev, G.M., Remizov, M.B., and Dubkov, S.A., *Vopr. Radiats. Bezopasn.*, 2004, no. 2 (34), pp. 15–23.
6. Martynov, K.V., Budantseva, N.A., Tananaev, I.G., et al., *Vestn. Otd. Nauk Zemle Ross. Akad. Nauk*, 2011, vol. 3, NZ6072, doi: 10.2205/2011NZ000202.

7. Glagolenko, Yu.V., Drozhko, E.G., and Rovnyi, S.I., *Vopr. Radiats. Bezopasn.*, 2006, no. 1, pp. 23–34.
8. Minaev, A.A., *Radiokhimiya*, 1979, vol. 21, no. 1, pp. 28–33.
9. Mogus-Milanković, A., Gajović, A., Šantić, A., and Day, D.E., *J. Non-Cryst. Solids*, 2001, vol. 289, pp. 204–213.
10. De la Rochère, M., Kahn, A., d'Yvoire, F., and Bretey, E., *Mater. Res. Bull*., 1985, vol. 20, pp. 27–34.
11. Gusarov, V.V., Mikirticheva, G.A., Shitova, V.I., et al., *Glass Phys. Chem.,* 2002, vol. 28, no. 5, pp. 309–316.
12. Masquelier, C., d'Yvoire, F., Bretey, E., et al., *Solid State Ionics*, 1994, vol. 67, pp. 183–189.
13. Lin, Y., Zhang, Y., Huang, W., et al., *J. Non-Cryst. Solids*, 1989, vol. 112, pp. 136–141.
14. Yu, X., Day, D.E., Long, G.J., and Brow, R.K., *J. Non-Cryst. Solids*, 1997, vol. 215, pp. 21–31.
15. Joseph, K., Premila, M., Amarendra, G., et al., *J. Nucl. Mater*., 2012, vol. 420, pp. 49–53.
16. Lai, Y.M., Liang, X.F., Yang, S.Y., et al., *J. Mol. Struct*., 2012, vol. 1013, pp. 134–137.
17. Ma, L. and Brow, R.K., *Am. Ceram. Soc. Bull*., 2013, vol. 92, pp. 36–39.
18. Kolesova, V.A., *Opt. Spektrosk.*, 1957, vol. 2, no. 2, pp. 165–173.
19. Lazarev, A.N., Mirgorodskii, A.P., and Ignat'ev, I.S., *Kolebatel'nye spektry slozhnykh okislov* (Vibration Spectra of Complex Oxides), Leningrad: Nauka, 1975.
20. Rokita, M., Handke, M., and Mozgawa, W., *J. Mol. Struct*., 2000, vol. 555, pp. 351–356.
21. Qian, B., Liang, X., Yang, S., et al., *J. Mol. Struct*., 2012, vol. 1027, pp. 31–35.
22. Makhakhas, Y., Aqdim, S., and Sayouty, E.-H., *J. Mater. Sci. Chem. Eng*., 2013, vol. 1, pp. 1–6.
23. Qian, B., Liang, X., Wang, C., and Yang, S., *J. Nucl. Mater*., 2013, vol. 443, pp. 140–144.

Translated by G. Sidorenko